The effects of using two color nonlinear plasmonic fields on increasing the cut off harmonics in attosecond pulses

Mostafa Ghadiri Soofi[1], Saeed Batebi*[2]

1 Department of faculty of science, university of Guilan, Rasht, Iran
, (+98) 9119434101. Mgh0141@yahoo.com
2 Department of faculty of science, university of Guilan, Rasht, Iran
, s_batebi@guilan.ac.ir

ABSTRACT

In present study, we investigated the production of a train of attosecond pulses, produced by plasmonic nanostructures. The field generated depended on the geometric shape of the nanostructure. Furthermore, the influence of strong two color laser inhomogeneous field on the creation of high-order harmonics was studied; this inhomogeneous was accompanied by increases in the cutoff frequency. Varying the parameters of the inhomogeneous structure also had a direct effect on the creation of the attosecond pulse. Moreover, we obtained pulses by using phase packets of sinusoidal quadrates. Our model was based on the numerical solution of the time-dependent (one-dimensional, (1D)) Schrödinger equation, and used classical and semi-classical calculations.

Key words: 1D time dependent Schrödinger equation, high order harmonic generation, isolated attosecond pulse, plasmonic field

Corresponding Author: Saeed Batebi

INTRODUCTION

Creating a HHG, which is one of the most important indicators of the nonlinearity of the interaction of strong laser fields with materials, has attracted significant attention for many years. The creation of such a train was predicted in the mid-1990s [1], and corresponding

experimental studies started a few years later [2, 3]. Furthermore, creating high-order harmonics based on convergent light supplies provides comprehensive insights into the temporal and spatial properties, with angstrom and attosecond precision.

The interaction with a single atom may be described by two model 1. semi-classical models 2. full quantum theory's [3, 4]. In the numerical solution applied to gaseous helium, the solution for the single atom is calculated by using the time-dependent Schrödinger equation. High-order harmonics are created by using a three-step semi-classical model [4]. According to this model, electrons, which do not possess kinetic energy, will become connected through tunneling ionization. The free electron is then accelerated in an oscillating electric field, until being restored either to an anion or initial molecule through the action of a laser field. Finally, during this return, the electron interacts with the open nucleus, and a high energy photon radiates; the energy of this photon is equal to the sum of the kinetic energy and the electron ionization potential. The diffusion model constitutes the classical component while the ionization and recombination processes are described using quantum mechanics. We obtain the ponder motive energy of the free electron in a laser field with intensity I and frequency ω, by using the maximum energy of the photon ($E_{\text{cut off}}$), where $E_{\text{cutoff}} = I_p + 3.17U_P$, I_P is the atomic potential, and $U_P = \frac{e^2E^2}{4m_e\omega^2}$ is the ponder motive energy which is the cycle averaged kinetic energy of an electron in a laser field[4].

A high-intensity laser field is required for the production of high-order harmonics. In recent years, many techniques, including the use of plasmonic fields [5, 6], have been suggested for the production of high-order harmonics [7]. In fact, plasmonic resonance nanostructures, which are the same as a light amplifier, were recently used to create these harmonics.

Each of these nanostructures can act as a point source, which produces plasmonic fields. Consequently, laser electric fields may be increased locally by up to 20 db [3, 9] by introducing rare gases, which have an intensified plasmon surface. Free electrons in the plasmonic plates result in a >100-fold increase in the intensity of the pulses, which in turn, leads to the production of high-order harmonics without a reduction of the repetition rate [8,12,13]. In such a system, the local intensity of the field is sufficiently increased and is even larger than the threshold intensity in rare gases required for the production of high-order harmonics. When a femtosecond low-intensity pulse is coupled with the plasmon mode and oscillates continuously between free charges of the metal, then the internal field resonance near the nanostructure is increased and high-order harmonics are eventually produced. This increase is higher than the threshold intensity needed to produce these harmonics in the rare gases. Consequently, artificial plasmonic fields may be used to produce HHGs, without an additional cavity or laser blowing process. Furthermore, the increased fields are spatially homogeneous at electron dynamic sites [10, 11]. In the following section, the time-dependent Schrödinger equation will be used for the numerical calculation of the HHG by integrating the real form of the electric field function near a bowtie-like metal nanostructure.

MATERIALS AND METHODS

For a linearly polarized field, as in the case of our study, the solution is obtained by solving the one-dimensional time-dependent Schrödinger equation (TDSE) based on the single-active electron approximation [14, 15,16]. (We use atomic units in all of the following equations),

$$i\frac{\partial\psi(x,t)}{\partial t} = \left[\hat{H}_0 + V_A(x) + V_L(x,t)\right]\psi(x,t) \Longrightarrow i\,|\,\dot{\psi}(x,t)\rangle = H\,|\,\psi(x,t)\rangle \quad (1)$$

Where $\hat{H}_0$ is the Hamiltonian in the absence of external fields, and $V_A(x)$ is the atomic potential. Here we use the "soft-core" potential for $V_A(x)$ and $V_L(x, t)$ represents the potential resulting from the laser electric field ($E(x, t)$) [17]. For the He atom,

$$V_L(x, t) = E(x, t).\, x \quad (2)$$

$$V_A(x) = -2/\sqrt{x^2 + 0.5} \quad (3)$$

In Eq. (2), the spatial dependency of $E(x, t)$ can be defined in terms of a perturbation of the dipole approximation; i.e.,

$$E(x,t) = E_0 f_1(t)\big(1 + H(x)\big).\sin(\omega_1 t + \varphi_1) + E_1 f_2(t)\big(1 + H(x)\big).\sin(\omega_2 t + \varphi_2) \quad (4)$$

$$H(x) = \sum_{i+1}^{N} a_i x^i \quad (5)$$

In Eq. (4), ω, $f(t)$, and φ are the frequency of the coherent electromagnetic radiation, pulse envelope, respectively. The linear polarization was performed along the x-axis. In addition, $H(x)$ represents the functional form of the inhomogeneous electric field and may be expressed as a power series, as shown in Eq. (5),
where the coefficients a_i are obtained by fitting the actual electric field that results from a finite element simulation, which considers the real geometry of different nanostructures [18]. The envelope function is then given as,

$$f(t) = sin^2\left(\frac{\omega_i t}{2n_p \pi}\right) \quad (6)$$

n_p is the number of plateau cycles and i = 1, 2.
Equation (1) is solved numerically by using the Crank-Nicolson scheme [19]. Moreover, the time-dependent induced dipole acceleration is determined from Ehrenfest's theorem [20]; i.e.,

$$d(t) = \frac{d^2\langle x\rangle}{dt^2} = -\langle\psi(x,t)\big|\big[H(t),[H(t),x]\big]|\,\psi(x,t)\rangle \quad (7)$$

Where, $H(t)$ and $\psi(x, t)$ are the Hamiltonian and the electron
$I(\omega)$ is obtained from the Fourier transformation of the time-dependent
Dipole acceleration $d(t)$,

$$I(\omega) = |d_\omega|^2 = \left|\frac{1}{\sqrt{2\pi}}\int d(t)e^{-i\omega t}\,dt\right|^2 \quad (8)$$

Attosecond pulses can then be generated by superimposing the harmonics,

$$I(t) = \left|\sum_{\omega} d_{\omega} e^{i\omega t}\right|^2 \quad (9)$$

Where $d_{\omega} = \int d(t)e^{-i\omega t}\, dt$ is the result of the inverse Fourier transformation [4].
In this work, the HHG power spectrum is calculated from a Fourier transformation of the dipole acceleration a(t); i.e.,

$$\mathrm{P}(\omega) = \left|\frac{1}{\sqrt{2\pi}} \int \mathrm{a(t)e^{-i\omega t}dt}\right|^2 \quad (10)$$

If an electron is ionized at t_i , then the corresponding emission time t_e can be obtained by solving the following equation,

$$\int_{t_i}^{t_e} \int_{t_i}^{t} E(t)dt = 0 \quad (11)$$

The kinetic energy E_k of an electron at t_i that returns to the parent ion at t_e can then be expressed as,

$$E(k) = \frac{1}{2}\left[\int_{t_i}^{t_e} E(t)dt\right]^2 \quad (12)$$

By solving Eqs. (11) and (12), we can examine the electronic dynamics of the HHG process in the synthesized field [21].
We begin by examining the role of the terms of the H(x) series, and hence, we express the linear term of the series for h(x) as,

$$E(x,t) = E_0 f(t)(1+ax).\sin(\omega_1 t + \varphi_1) + E_1 f(t)(1+ax).\sin(\omega_2 t + \varphi_2) \quad (13)$$

The non-linear term of the series for h(x) is,

$$E(x,t) = E_0 f(t)(1+ax+ax^2).\sin(\omega_1 t + \varphi_1) + E_1 f(t)(1+ax+ax^2).\sin(\omega_2 t + \varphi_2) \quad (14)$$

Where "a" is a parameter that characterizes the strength of the linear and non-linear inhomogeneous and has dimensions of inverse length; we also set I = 10^{13} and $2 \times 10^{14}\, w/cm^2$ and used a sinusoidal-shaped pulse with one optical cycle, and a plateau of constant-amplitude optical cycles ($n_p = 4$) .we used He gas for our research.

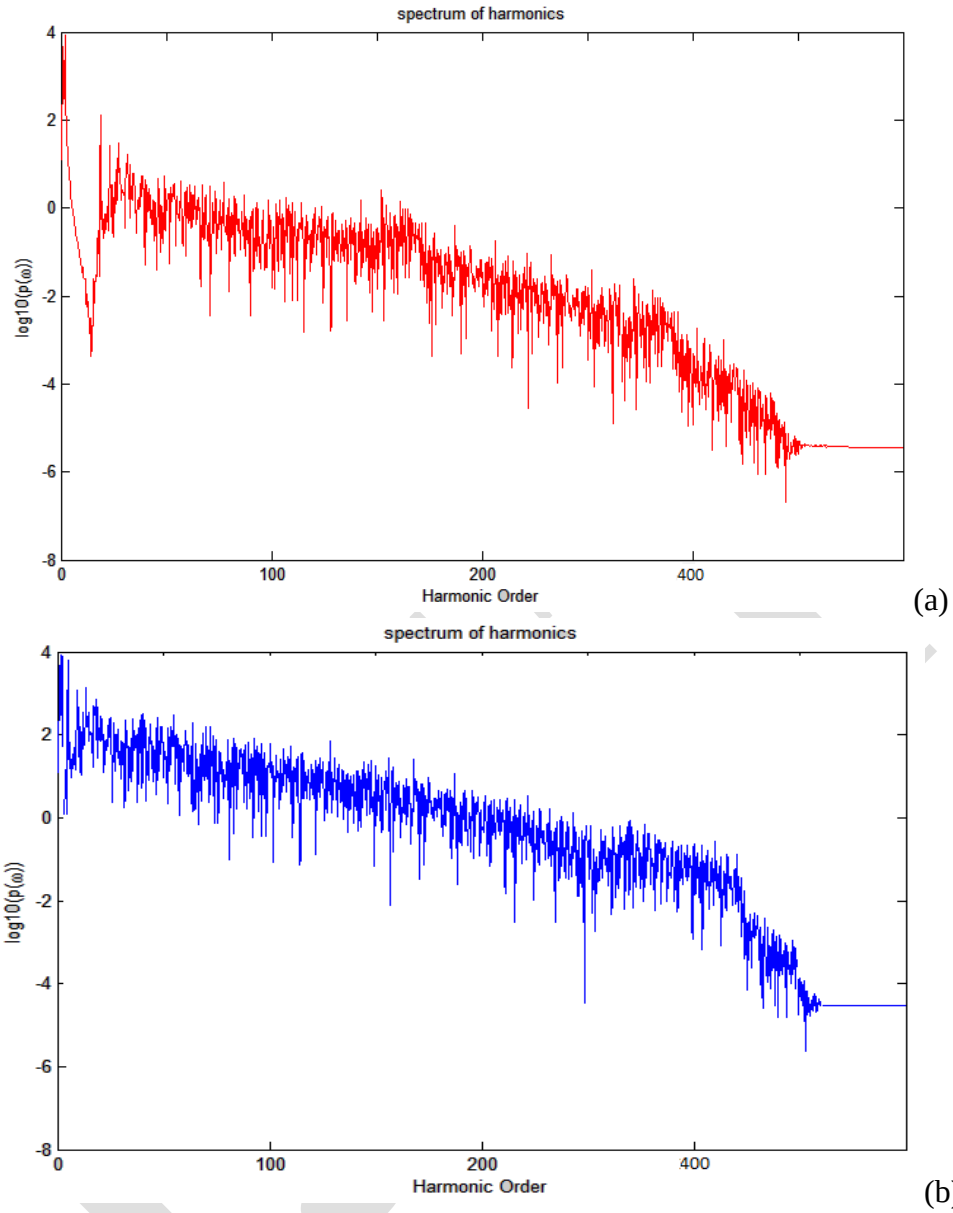

Fig. 1. (a) High-order harmonic generation (HHG) spectra for a He gas with $E_{GS} = -0.58$ a.u. generated using the 1D_TDSE. The laser parameters are I = 10^{13} and 2×10^{14} w/cm^2, $\varphi_1 = \pi/2$, $\varphi_2 = \pi/2$, and λ = 800 nm. We used a pulse with four optical cycles for a = 0.003 (red) in linear inhomogeneous H(x) mode. (b) a = 0.003 (red) in non-linear inhomogeneous H(x) mode.

Harmonic spectra with linear ad non-linear H(x) of the fundamental and sub-harmonic pulses are shown in Fig.1 (a) and 1(b), respectively. The harmonic spectrum in Fig.1 (a) exhibits the typical plateau structure. This irregular plateau begins with a few initial harmonics, is followed by smooth and continuous plateaus, and ends with a sharp cutoff. We examined the linear H(x) behavior, based on Eq. (13), i.e., we used a pulse with four optical cycles, for a = 0.003. We also used the $E(x,t)$ from Eq. (14), i.e., the non-linear H(x), and obtained a similar result (Fig.

1(b)) to that shown in Fig. 1(a) for a = 0.003 . Fig. 1(a) and 1(b) also reveal that the ratio of the H(x) increased the cutoff point. the orders of the cutoff are 395th (in 1(a)) and 450th (black line in 1(b)) for linear and non-linear homogeneous, respectively. Comparing these results reveals that the cutoff order can be increased by using an enhanced field and by the inhomogeneous parameter, especially in the case of non-linear homogeneous. The increased order of the cutoff results in an attosecond pulse, which is the shortest pulse obtained in this study. The aforementioned results also show that the HHG is highly sensitive to the plasmonic of both the fundamental and sub-harmonic control pulses.

Figure 2 shows the temporal profiles of the attosecond pulses, obtained by filtering the intense super continuous harmonics. By selecting harmonics of the 340th–400th order (black) and of the 425th–480th order (blue), the corresponding duration of the intense isolated pulses can be determined. We then compared the linear and non-linear behavior of H(x). Figure 2 shows the

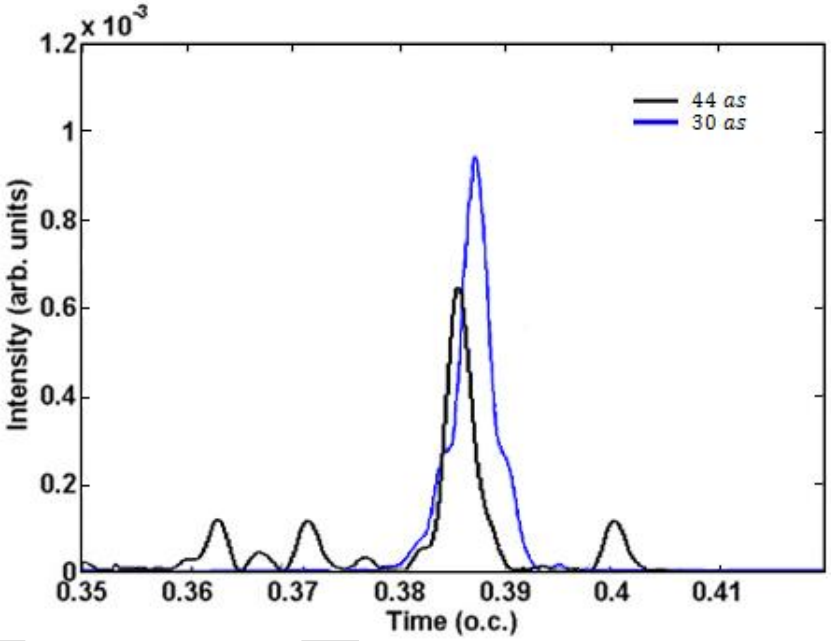

Fig. 2. (Color online) The isolated attosecond pulse in the linear inhomogeneous, for a = 0.005 (black), obtained by superimposing 320th–420th order harmonics; this superposition resulted in a 44 attosecond pulse; in the case of the non-linear inhomogeneous, a = 0.005 (blue), a 30 attosecond pulse was obtained by superimposing the 420th–487th harmonics.

Profile pulse generated for a = 0.005 (black) and a = 0.005 (blue) for linear and non-linear inhomogeneous, respectively. The linear and non-linear inhomogeneous resulted in single, isolated 44 as and 30 as pulses, respectively. Figure 2 makes clear that the inhomogeneous parameter results in increased order of the cutoff. In fact, changing the inhomogeneous of H(x) from linear to non-linear leads to significant increases in the cutoff order.

Figure 3 shows the corresponding time–frequency distributions of HHG. The distribution in Fig. 3(a) exhibits two main peaks with maximal harmonic orders of 195 and 390. Figure 3 shows that for the high-order harmonics, the contribution of the long quantum path is substantially more intense than that of its short quantum counterpart. The short quantum path leads to

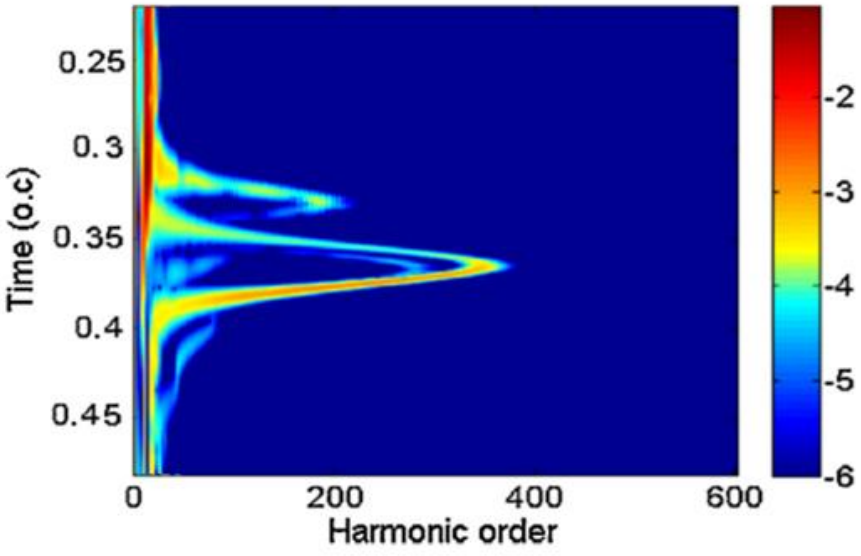

(a)

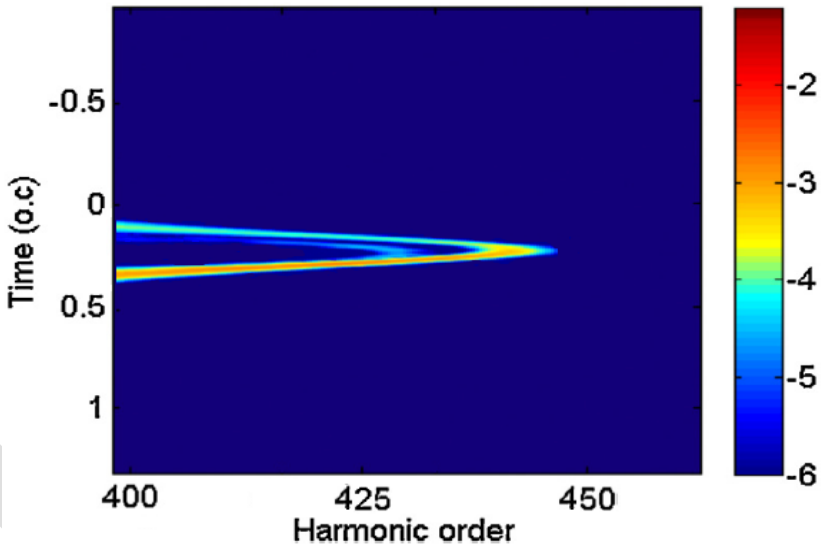

(b)

Fig. 3. The time–frequency distribution of the blue solid curve in Fig. 3 for a = 0.005 and in the case of (a) linear inhomogeneous and (b) nonlinear inhomogeneous. (For interpretation of the references to color in this sentence, the reader is referred to the web version of the article.)

the slight modulation of the HHG spectrum in the plateau. There is only one long quantum path for harmonics of the 200^{th}–390^{th} order, while the short trajectory is mainly suppressed, leading to the generation of a broad band super continuum spectrum. The harmonic efficiencies of the long paths in (b) are therefore significantly higher than those in (a).

CONCLUSION

When we use inhomogeneous field, the cutoff of spectrum is extended. Also by increasing the value of H(x) parameter, the cutoff order increased. By superposing several consecutive harmonics of this part, a single isolated attosecond pulse produced by ideal time profile. Although by changing the inhomogeneous of H(x) from linear to non-linear leads to significant increases in the cutoff order.

REFERENCE

[1] Krausz F and Ivanov M 2009 Rev. Mod. Phys. 81 163.
[2] Dombi P et al 2010 Opt. Express 18 24206.
[3] kim S et al, Nature 435 757 (2008)..
[4] mojtaba T et al,Ijer 543-545(2014).
[5] Uiberacker M et al, Nature 446 627 (2007).
[6] Schultze M et al, Science 328 1658 (2010).
[7] M. Mohebbi, S. Batebi / Journal of Electron Spectroscopy and Related Phenomena 185 (2012) 578– 587
[8] Goulielmakis E et al, Nature 466 739 (2010).
[9] P.B. Corkum, Phys. Rev. Lett. 71 (1993) 1994.
[10] I.-Y. Park, S. Kim, J. Choi, D.-H. L. Y.-J. Kim, M. F.Kling, M. I. Stockman, and S.-W. Kim, Nat. Phot. 5,677 (2011).
[11] P. M¨ uhlschlegel, H.-J. Eisler, O. J. F. Martin, B. Hecht, and D. W. Pohl, Science 308, 1607 (2005).
[12] Sansone G et al, Nature 465 763 (2010).
[13] Cavalieri A et al, Nature 449 1029 (2007).
[14] M. Lewenstein, P. Balcou, M. Y. Ivanov, A. L'Huillier, and P. B. Corkum, Phys. Rev. A 49, 2117 (1994).
[15] R.F. Lu, H.X. He, Y.H. Guo, K.L. Han, J. Phys. B: At. Mol. Opt. Phys. 42, 225601
[16] C. Figueira de Morisson Faria, M. Dörr, W. Sandner, Phys. Rev. A 55, 3961 (1997).
[17] C. Figueira de Morisson Faria, M. Dörr, W. Sandner, Phys. Rev. A 58, 2990 (1998).
[18] M. F. Ciappina, T. Shaaran, and M. Lewenstein, Physics.atom-ph. Arxiv: 1210.5610v1.
[19] M. Protopapas, C. H. Keitel, and P. L. Knight, Rep. Prog. Phys. 60, 389 (1997).
[20] Q. Su and J. H. Eberly, Phys. Rev. A 44, 5997 (1991).
[21] M. Mohebbi, S. Batebi, Optics Communications 296 (2013) 113–123.